

# Mesospheric Temperature and Ozone Sounding by the SMAS Solar Occultation Sensor

Christoph Rehl and Gottfried Kirchengast  
Institute for Geophysics, Astrophysics, and Meteorology (IGAM)  
University of Graz, Graz, Austria

UNI  
GRAZ



## Introduction

Absorptive occultation data bear great capability of providing profiles of atmospheric key quantities like temperature and trace gases such as ozone. The unique Sun Monitor and Atmospheric Sounder (SMAS) sensor concept uses an active limb sounding technique with the sun as the source of light and high-precision UV photometers as detectors in LEO (Low Earth Orbit). The Earth's atmosphere in between acts as the absorbing medium, whereby SMAS primarily aims at mesospheric profiles of temperature and ozone (on the basic concept and original proposal of SMAS see Kirchengast et al., 1998).

SMAS provides, based on high-precision photodiode sensors, self-calibrated transmission data in 14 UV channels within 1-250 nm (6 EUV channels within 1-130 nm and 8 MUV channels within 180-250 nm) and in one 300-700 nm VIS broadband channel, respectively. While the 6 EUV channels allow to obtain profiles of molecular oxygen, molecular nitrogen, atomic oxygen, and temperature in the thermosphere (above 100 km), the 8 MUV channels allow to accurately retrieve ozone and temperature profiles in the mesosphere. We focus in the present work on use of the MUV channels.

## SMAS Channel Selection

To provide mesospheric ozone and temperature profiles, the SMAS sensor uses the middle UV wavelength region. This is the most important spectral realm of interaction of the upper middle atmosphere with the incoming solar radiation. SMAS exploits the limb attenuation due to absorption for analyzing the atmosphere. The intensity of the solar radiation passing the Earth's middle atmosphere is given by the combined attenuation of all absorbing species along the ray path and can be basically determined using the Bouguer-Lambert-Beer law, at each frequency  $\nu$ , in the form

$$T_\nu = \frac{I_\nu(s)}{I_\nu(0)} = \exp \left[ - \int_{sun}^{leo} \sum_i n_i(s) \sigma_{i\nu}(s) ds \right]$$

The normalized transmission  $T_\nu$  at any given frequency is a ratio of the solar radiation intensity measured in the atmosphere,  $I_\nu(s)$ , relative to the solar intensity above the atmosphere,  $I_\nu(0)$ , measured at top of the atmosphere. The integral is carried out along a ray path  $s$ , the ray path is slightly refracted for altitudes up to about 75 km, above refraction and thus bending of the rays is negligible. The number densities  $n_i$  and cross sections  $\sigma_{i\nu}$  are associated with the primary mesospheric absorbers, molecular oxygen and ozone. Figure 1 includes a summary table on the relevant channels and illustrates optical thickness properties. The instrumental bandwidth of the MUV channels is 5 nm, which is at present the technical optimum given by the FIPM Freiburg, Germany (the SMAS hardware developers; cf. Rieder and Kirchengast, 2001).

Channel Number	Channel Wavelength [nm]	Solar origin of radiation	Main solar emission	Atmospheric species intervening in occultation
1 (EUV)	1-10	Corona		N <sub>2</sub> , O <sub>2</sub> , O
2 (EUV)	17-25	Corona	Fe X - Fe XII	N <sub>2</sub> , O
3 (EUV)	29-35	Transition region	He II (30.4 nm)	N <sub>2</sub> , O
4 (EUV)	50-65	Chromosphere	He I (66.8 nm)	N <sub>2</sub> , O
5 (EUV)	70-90	Transition region	O I - O IV	N <sub>2</sub> , O
6 (EUV)	110-130	Chromosphere	H I (121.6 nm)	O <sub>2</sub>
7 (MUV)	184.2-5	Photosphere	Continuum	O <sub>2</sub>
8 (MUV)	190.2-5	Photosphere	Continuum	O <sub>2</sub>
9 (MUV)	195.2-5	Photosphere	Continuum	O <sub>2</sub> , O <sub>3</sub>
10 (MUV)	200.2-5	Photosphere	Continuum	O <sub>2</sub> , O <sub>3</sub>
11 (MUV)	205.2-5	Photosphere	Continuum	O <sub>2</sub> , O <sub>3</sub>
12 (MUV)	210.2-5	Photosphere	Continuum	O <sub>2</sub> , O <sub>3</sub>
13 (MUV)	224.2-5	Photosphere	Continuum	O <sub>2</sub>
14 (MUV)	240.2-5	Photosphere	Continuum	O <sub>2</sub>
15 (VIS)	300-700	Photosphere	Continuum	Air

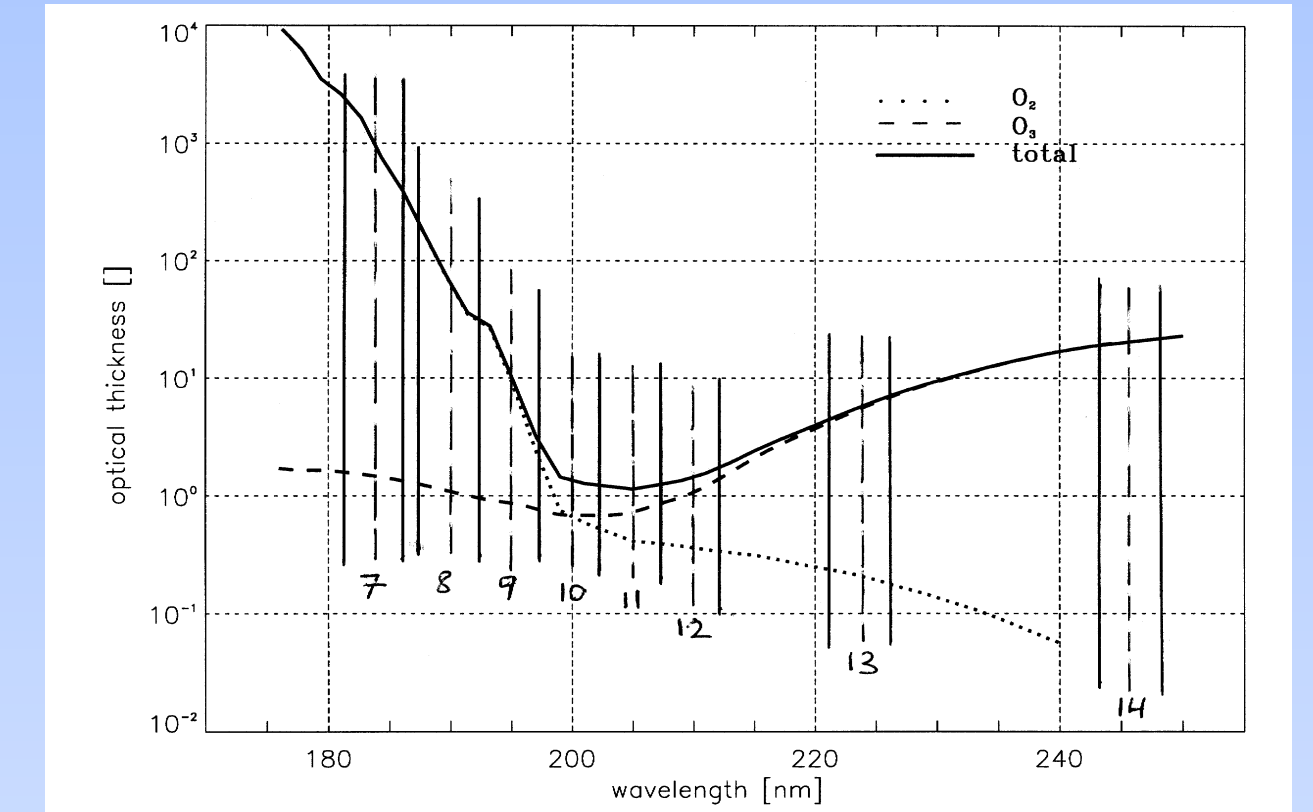


Fig. 1: Channel selection for the SMAS sensor concept (left panel) and typical optical thickness of molecular oxygen, ozone, and both together within 170 nm and 250 nm at a height of 60 km (right panel). The wavelength locations of the mesospheric SMAS channels (channels 7 to 14) are also visualized in the right panel. The locations of the 8 channels are defined such that a proper transmission coverage of the whole mesosphere is ensured.

The examination of the radiative interaction properties of the Earth's atmosphere leads to a natural range in the UV wavelength region  $< 250$  nm. For the most needed height range complementary to GOMOS on ENVISAT (60-100 km), the best spectral regions for molecular oxygen/temperature are the Schumann-Runge (SR) bands (175-204 nm) and the Herzberg continuum (185-242 nm). For ozone, the short-wavelength part of the Hartley band (200-310 nm; maximum at 250 nm) is the spectral region of interest. For details on relevant cross-sections see, e.g., Minschwaner et al. (1992) and Molina and Molina (1986).

## SMAS Transmission

The full observed transmission can be modeled as function of sampling time  $t_i$

$$T(t_i) = \int_{\Delta t} \int_{\Delta \nu} \int_{\Delta \lambda} T_{am}(\lambda, \nu, t) W(\lambda - \lambda_0) W_\nu W_\lambda d\lambda d\nu dt$$

The baseline sampling rate is 10 Hz. The integral is carried out over the wavelength region  $\lambda$ , and the field of view  $\nu$  (1/30 deg). Characteristic limb transmission profiles  $T_{am}$  results from the well known geometry.  $W(\lambda - \lambda_0)$  is a Gaussian channel shape function,  $W_\nu$  and  $W_\lambda$  are "boxcar" functions for field-of-view and integration time. An exact calculation in the SR bands needs a resolution of 3000 sampling points (0.002 nm) for each channel. The strongly temperature dependent SR absorption cross sections are shown in Figure 2, left panel, the right panel illustrates the SMAS transmission profiles. In the Herzberg region, a resolution of 30 sampling points (0.2 nm) is sufficient, due to the smooth behavior of the cross sections and the negligible temperature dependence. Due to the dense sampling in the SR bands, a relatively slow exact forward model algorithm results - to obtain a fast SR algorithm we used following approximations.

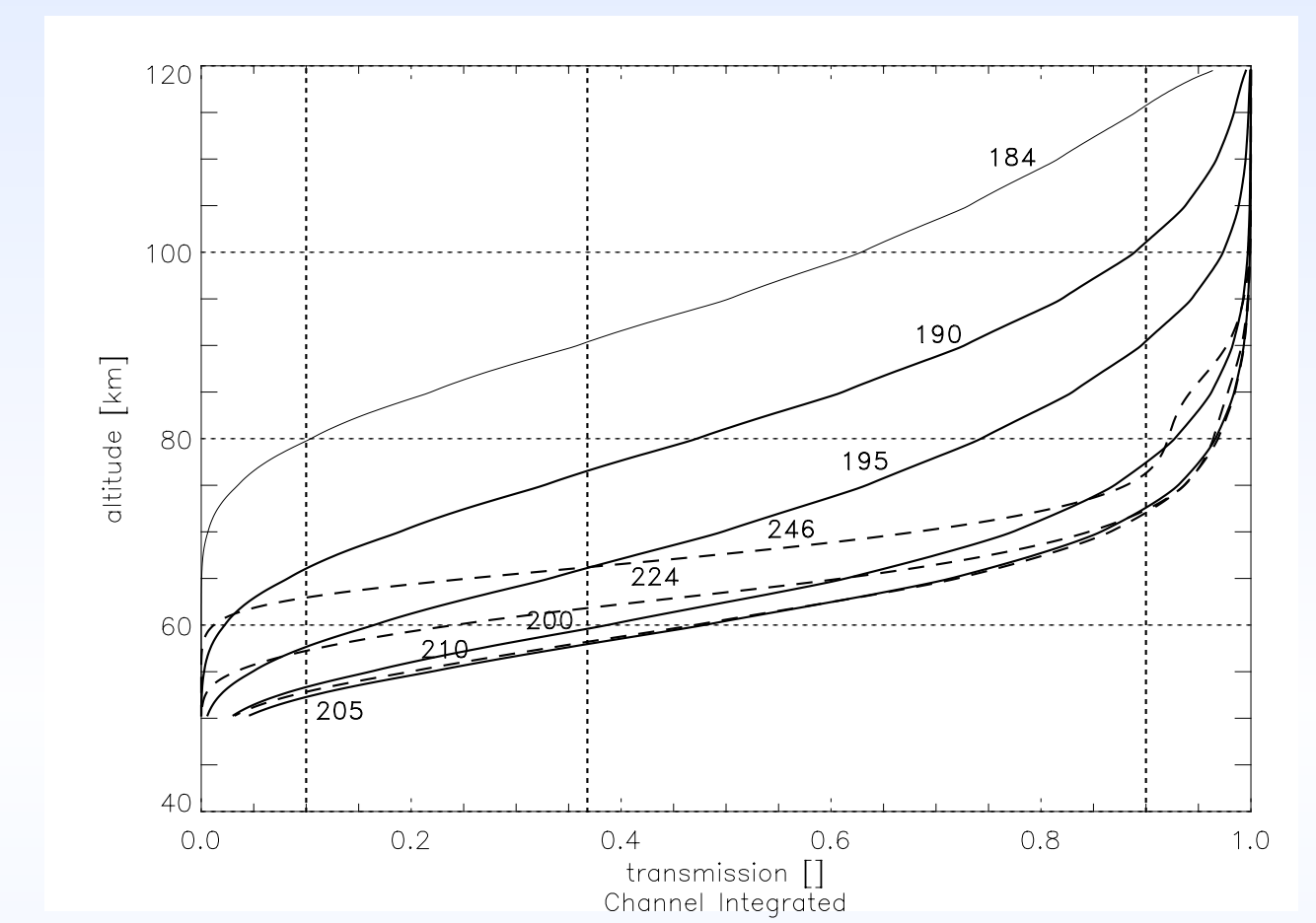
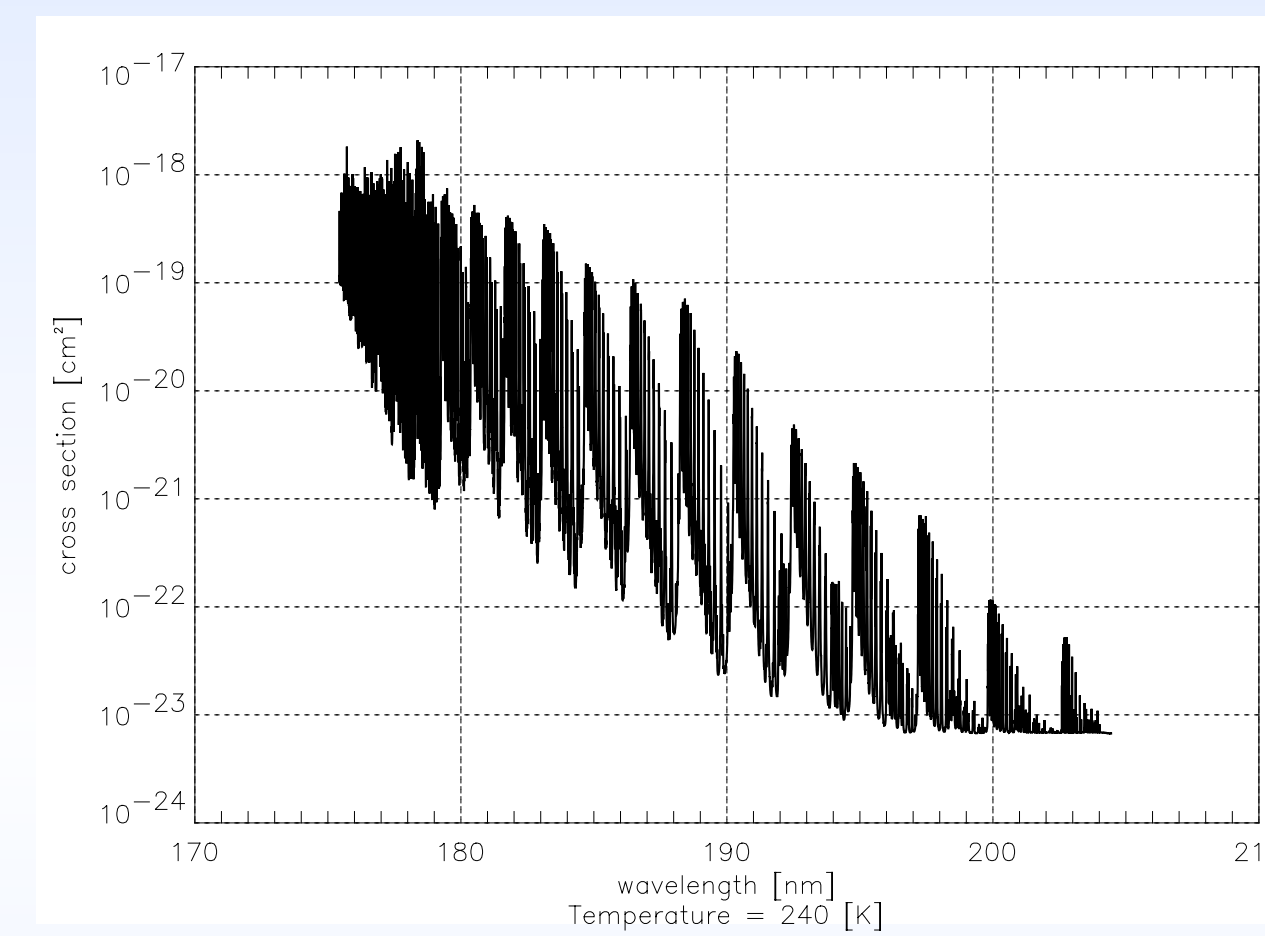


Fig. 2: Spectral distribution of the absorption cross section of molecular oxygen in the SR bands (left panel) and modeled SMAS transmission profiles (right panel). The solid lines show the transmission in the SR bands and the dashed lines the ones in the Herzberg continuum and overlapping Hartley band (the annotated numbers show the channel center wavelength). The dashed verticals at 0.1 and 0.9 indicate the region within measurements shall be exploited.

## i) Optimal Random-Selection Approximation (ORSA)

In the ORSA, the 3000 sampling bins per SR channel are reduced by Monte-Carlo drawings ( $10^4$  trials) to a random subset of 100 bins, which is optimal for a given atmospheric condition in producing the most accurate channel transmission profile among all trials (compared to the exact forward model). Performing this ORSA selection of 100-bin subsets for a sufficient diversity of atmospheric conditions (temperature profiles) provides a number of look-up tables, used in a nearest-neighbor sense, for a fast algorithm based on only 100 bins per SR channel. A set of 18 conditions seems sufficient for the purposes of SMAS.

## ii) Piecewise - Integration Approximation (PIA)

In the PIA, cross sections integrated over a finite equidistant wavelength range, starting at the lower wavelength boundary up to the upper wavelength boundary of each SMAS SR channel, are used to calculate the SR transmissions, weighted by the averaged Gaussian channel shape function. A set of at least 300 such spectrally-averaged bins leads to an acceptable precision. Figure 4 compares the performance of the ORSA and the PIA for an exemplar case. The relative differences between the true and by random selection (left panel), and piecewise integrated (right panel) respectively approximated transmission profiles are shown in Figure 4.

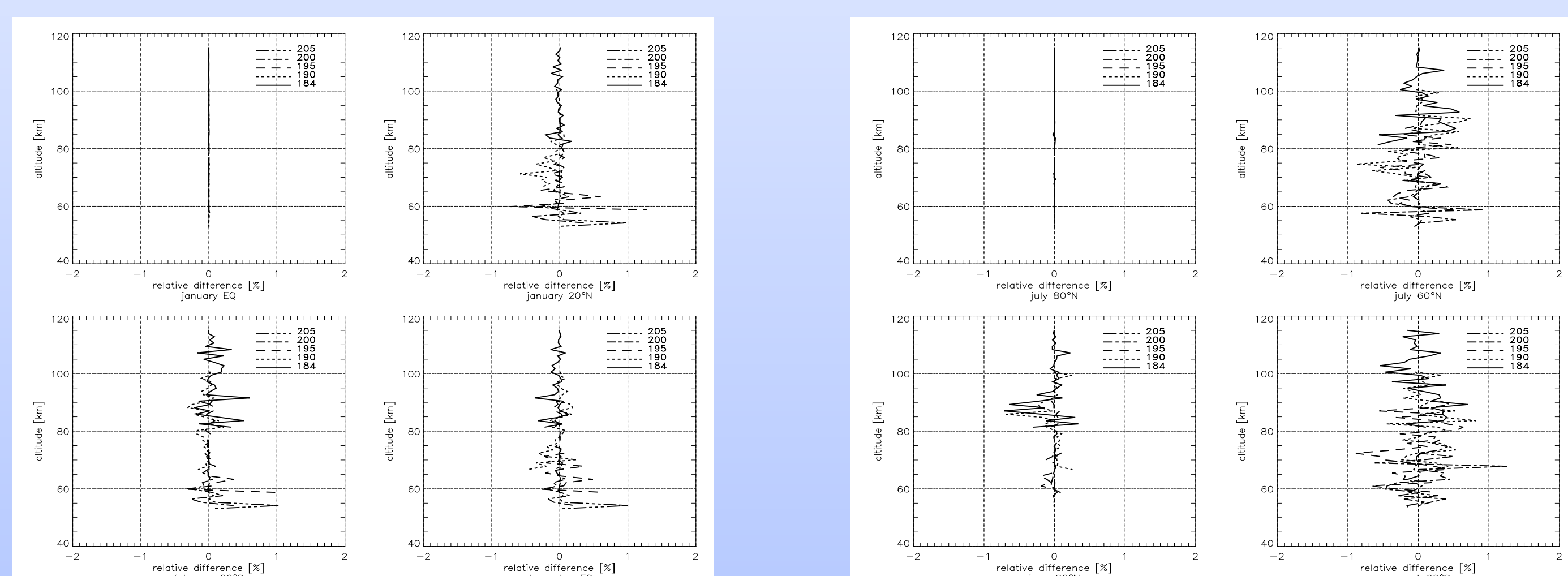


Fig. 3: Illustration of ORSA performance for a few exemplary atmospheric conditions (CIRA86 profiles). Each sub-panel shows the accuracy of the ORSA with the exact forward model for the "true" conditions as reference. The upper-left sub-panels of the left and right panel show the baseline accuracy (i.e., ORSA directly based on "true" conditions), the others show the realistic situation, where the ORSA selection is based on "a priori" knowledge of conditions only.

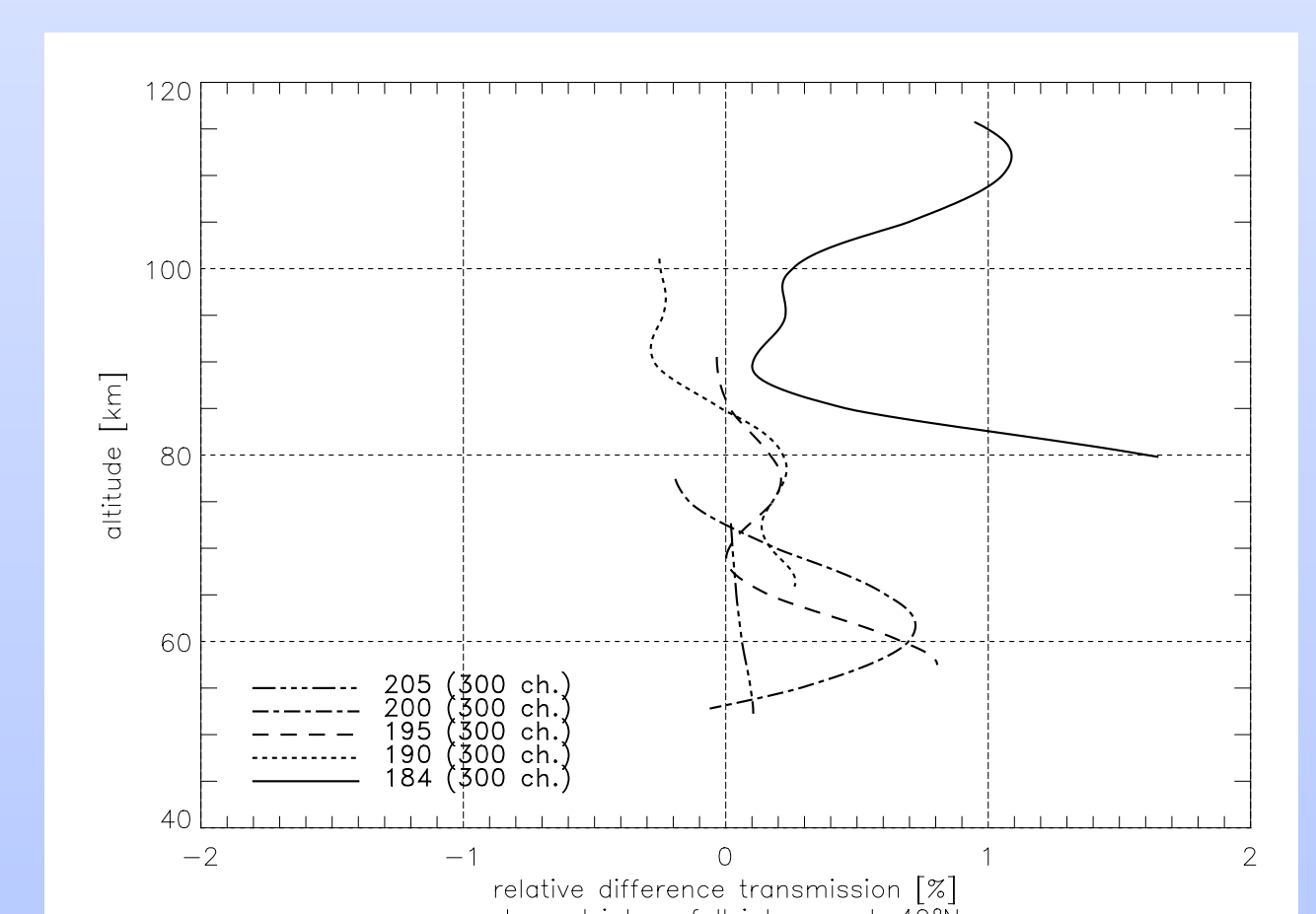
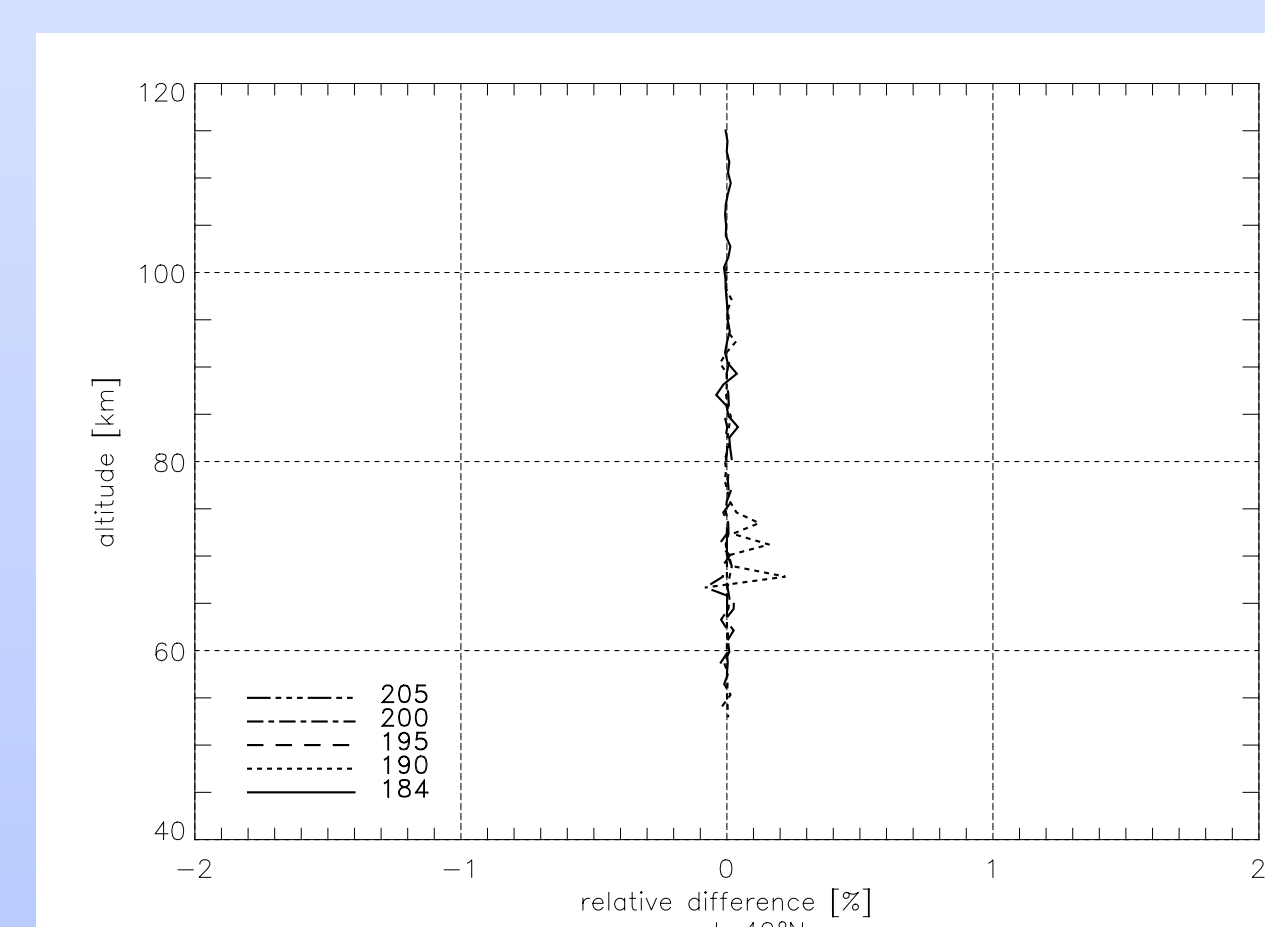


Fig. 4: Accuracy of the ORSA (left panel) and the PIA (right panel) for a representative atmospheric condition (CIRA86, March, 40°N). Together with Fig. 3 this indicates that the ORSA with 100 bins leads to superior results than the PIA with 300 bins (with 100 bins, PIA significantly exceeds 1% errors).

## Results - Ozone Retrieval

While retrieval algorithm preparations for the SR channels are still on-going, first retrieval results already exist for the ozone channels, i.e., the ozone retrieval is based on the Hartley band channels only (SMAS channels 12, 13, 14; all three with smoothly varying cross sections). A sequential inversion process was applied, starting with a spectral inversion of transmissions to molecular oxygen and ozone columnar content profiles, followed by a vertical inversion to obtain an ozone number density profile.

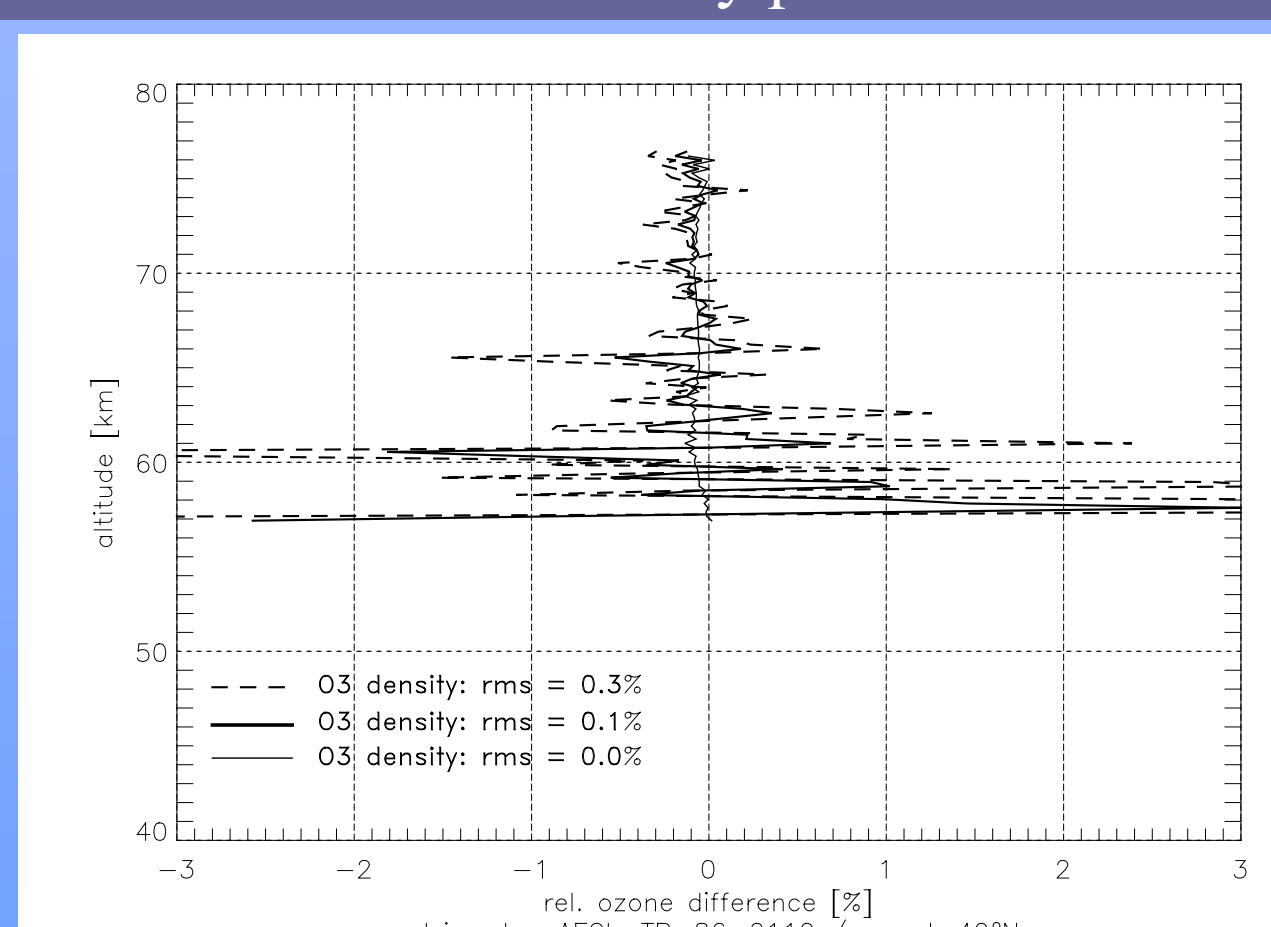
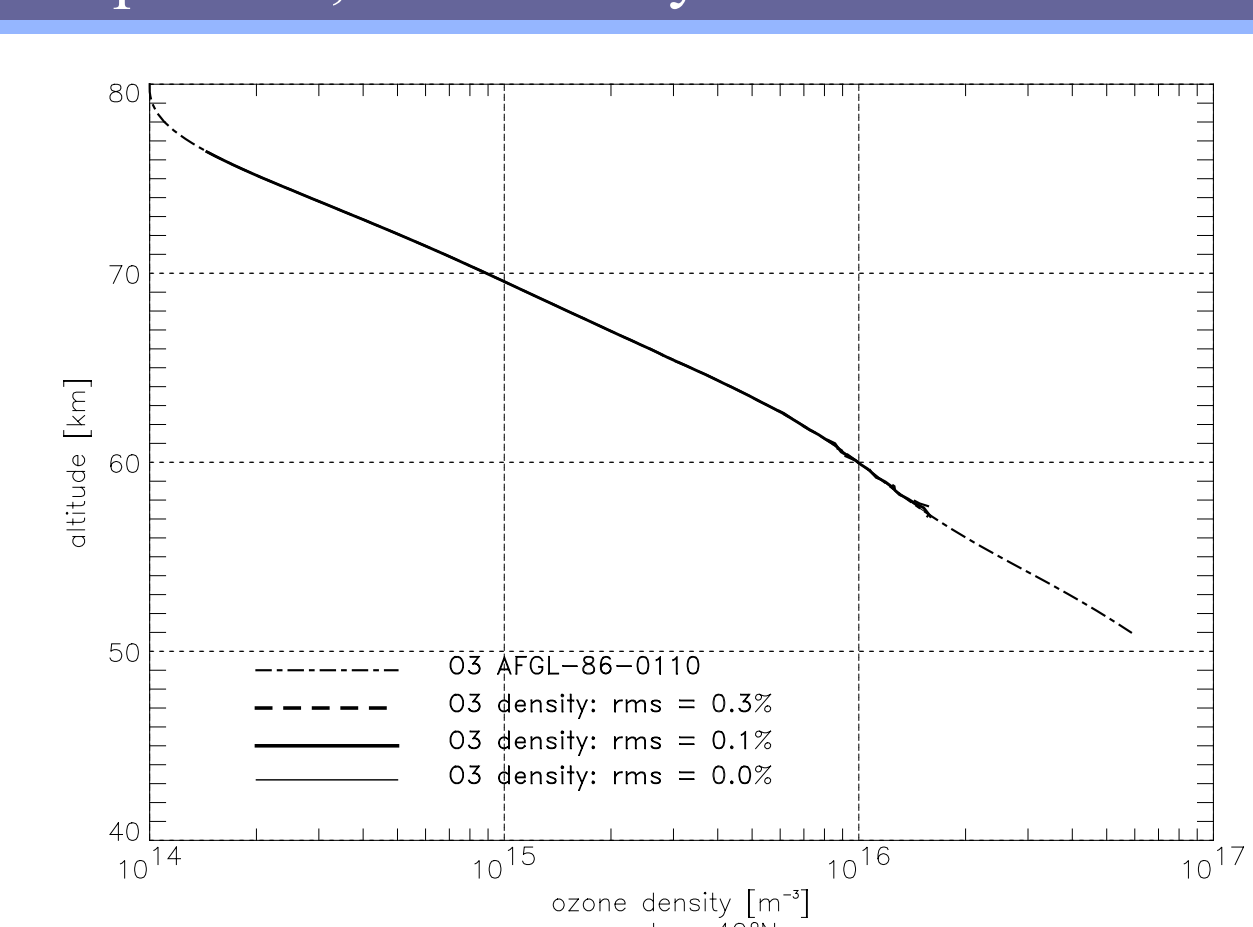


Fig. 5: SMAS-retrieved ozone profile (left panel) and relative difference between retrieved profiles and true profile for different sensor noise levels (right panel). A standard (AFGL) mid-latitude ozone profile was used as "true" profile.

Regarding the vertical inversion, the Abel integral was discretized into matrix form assuming linear variation of number densities in layers (cf. Syndergaard, 1999). Figure 5 shows, for an exemplary case, the retrieved ozone density profile (left panel) and relative differences between retrieved and true profiles (right panel). The sensor noise levels assumed for SMAS in this example were those used by Rieder and Kirchengast (2001) based on the hardware developer's specification: 0.1% rms error at 10 Hz sampling rate and unity transmission for diamond UV photodiodes (heavy solid line), and 0.3% for silicon diodes (dashed line), respectively; the height resolution provided is  $\sim 2$  km. The small residual for 0.0% error (light solid line) indicates residual numerical errors. The present preliminary results indicate that the SMAS sensor well enables mesospheric ozone retrieval accuracy of better than 1% down to about 60 km.

## References

- Kirchengast, G., M. Gorbunov, N. Jakowski, L. Kornbluh, U. Mallow, A. Rius, C. Rocken, M. Rothacher, G. Schmidtke, M. Sust, J. Ward, and A. Wernik, ACISCOPE - Atmosphere and Climate Sensors Constellation Performance Explorer (ESA Earth Explorer Opportunity Mission proposal), *Wiss. Ber. No. 4/1998*, 60pp., Inst. for Geophys., Astrophys., and Meteorology, Univ. of Graz, Austria, 1998.
- Minschwaner, K., G.P. Anderson, L.A. Hall, and K. Yoshino, Polynomial Coefficients for Calculations, *J. Geophys. Res.*, **97**, 10,103-10,108, 1992.
- Molina, L.T., and M.J. Molina, Absolute absorption cross sections of ozone in the 185 nm to 350 nm wavelength range, *J. Geophys. Res.*, **91**, 14,501-14,508, 1986.
- Rieder, M.J., and G. Kirchengast, Error analysis for mesospheric temperature profiling by absorptive occultation sensors, *Ann. Geophys.*, **19**, 71-81, 2001.
- Syndergaard, S., Retrieval analysis and methodologies in atmospheric limb sounding using the GNSS radio occultation technique, *DMI Sci. Rep. 99-6*, 131pp., Danish Meteorol. Inst., Copenhagen, Denmark, 1999.